Journal of Nuclear Materials 390–391 (2009) 925–928

Contents lists available at ScienceDirect

Journal of Nuclear Materials

journal homepage: www.elsevier.com/locate/jnucmat

# $CD_4$ production from mixed W–C–D surface during simultaneous irradiation of W with $C^+$ and $D^+$

I.A. Bizyukov [a], J.W. Davis [a], A.A. Haasz [a,*], P. Brodersen [b]

[a] University of Toronto Institute for Aerospace Studies, 4925 Dufferin Street, Toronto, Ontario, Canada M3H 5T6
[b] Department of Chemical Engineering and Applied Chemistry, University of Toronto, Canada

ARTICLE INFO

*PACS:*
28.52.Fa
79.20.Rf
82.45.Mp

ABSTRACT

Simultaneous irradiation of W was performed with 6 keV $C^+$ and 0.1–0.4 keV $D^+$ ion beams; the C fraction in the combined total flux was ~4%. Beam energies and fluxes were selected to provide continuous erosion of the mixed W–C–D surface, preventing the formation of a carbon overlayer. The temperature-dependent features of the methane production curves confirm the occurrence of chemical erosion from the mixed-material surface. In general, the curves exhibit the highest erosion rates at room temperature (~300 K) followed by a decreasing trend with increasing temperature. Methane yield ($CD_4/D^+$) estimates are ~1–1.5% at RT, decreasing to ~0.5% at 500 K, and levelling off at higher temperatures. XPS depth profiles confirm the depletion of C from the mixed W–C–D surface layer; however, at present we cannot determine what fraction of this is due to physical or chemical sputtering.



## 1. Introduction

The current ITER design calls for tungsten in the divertor baffle region and graphite (carbon–fibre composite) for the high-heat flux divertor plate [1–3]. During plasma operation, the W plasma-facing surfaces will be exposed to high fluxes of deuterium and tritium ions and neutrals, as well as various impurities, including carbon. Due to the vicinity of the carbon plates, it is anticipated that W erosion will be caused mainly by energetic C ions and neutrals [4,5]. Experiments in ASDEX Upgrade have shown that W surfaces erode mainly by C, O and W impurity ions [6]. Although, the main mechanism of W erosion is physical sputtering, there is uncertainty regarding the processes on the surface, which may affect the W sputtering yield.

Irradiation of W with $C^+$ and $D^+$ leads to the formation of a mixed W–C–D surface due to ion implantation and D retention. In addition to kinematic processes, chemical interactions between C and D may be involved, resulting in the formation and release of hydrocarbons. Previous studies have shown that the W sputtering yield from a mixed W–C–He surface is lower than that of pure W [7]. Moreover, under certain conditions $C^+$–$D^+$ irradiation may lead to surface erosion or, alternatively, to the formation of pure C layers. It has been shown by Schmid and Roth [8] that the combined irradiation of W with $H^+$ and $C^+$ (using $C^+$ and $CH_4^+$ ions) at high temperature (1073 K) leads to surface erosion rather than C deposition. It was suggested [8] that carbon is removed from the mixed surface via chemical erosion and diffusion, leaving a bare W surface exposed to impurity fluxes, which can lead to an increase in W sputtering. This in turn would increase the W influx into the plasma and reduce the lifetime of W plasma-facing materials.

The data on C chemical sputtering from mixed W–C–D surfaces is rather limited. Balden et al. [9] produced magnetron-sputtered C–W layers, which they subsequently irradiated with a single-beam of 30 eV/D ions over a wide temperature range. Their W concentrations in the C–W layers varied between 2.8 and 14.5 at.% [9]. However, the C/W ratio may vary in the range 0–100 at.% depending on the local incident flux. For example, for simultaneous irradiation of W with $C^+$ and $D^+$ beams, Bizyukov and Krieger [10] reported W concentrations of ~30 at.% and above in the top layer of the mixed surface. Another limitation of using only $D^+$ irradiation on the mixed C–W surface is the preferential sputtering of C, leading to continual changes in surface composition.

The objective of the present study was to investigate whether, and to what extent, chemical release of carbon occurs from a mixed W–C–D surface layer formed during simultaneous irradiation of W with independently controlled $C^+$ and $D^+$ ion beams – in the absence of a protective carbon 'overlayer' on top of the mixed W–C–D surface. (An excellent signature of chemical erosion is the formation of hydrocarbon reaction products – methane in particular.) The main advantage of the simultaneous irradiation approach is the ability to achieve stable surface conditions at fixed beam energies and fluxes.

* Corresponding author.
*E-mail address:* tonyhaasz@utias.utoronto.ca (A.A. Haasz).

0022-3115/$ - see front matter © 2009 Elsevier B.V. All rights reserved.
doi:10.1016/j.jnucmat.2009.01.237

## 2. Experiment

A single tungsten specimen was used in these experiments. It was cut from a hot-rolled 25 μm thick W foil (99.95 at.% pure) supplied by Rembar Company Inc. The frontal dimensions were $1 \times 4\ cm^2$. Prior to dual-beam irradiation the specimen was washed with ethanol and was pre-irradiated with $D^+$ while being heated at ~900 K to remove surface impurities by sputtering; 900 K was used to avoid D retention. The specimen was heated resistively and the temperature was monitored by a K-type thermocouple. The measurement accuracy was ~5 K at room temperature (RT), but we suspect that it was underestimated by up to 70 K at 900 K, due to the thermocouple being located a few mm away from the central part of the specimen. We have not corrected for errors in the thermocouple readings.

The specimen was irradiated with independently controlled and mass-analyzed beams of $C^+$ and $D_3^+$ using the UTIAS dual-beam ion accelerator [11]. The specimen was biased to achieve lower ion energies while maintaining acceptable ion fluxes. The $C^+$ energy was fixed at 6 keV while the $D_3^+$ energy was varied to produce 100–400 eV/$D^+$. (We denote the incident particles as $D^+$ even though not all atoms in the molecular $D_3^+$ ion are charged.) These energies correspond to a mean projectile range of 11 nm for $C^+$ in W and 4.3–9.2 nm for $D^+$ in W [12]. The angle of incidence for each ion beam was 21° from the surface normal, forming a 42° angle between the two beams.

The C fraction in the total incident flux was maintained at ~4%, while the total flux ($C^+$ plus $D^+$) was kept at $4 \times 10^{18}\ m^{-2}s^{-1}$. We note that the $C^+$ and $D^+$ beam diameters were ~4 mm and ~5 mm, respectively. The ~4 mm C spot diameter is consistent with the lateral spread of the X-ray photo-electron spectroscopy (XPS) C profiles shown in Fig. 1 (Similar carbon depth profiles are seen at different radial locations from bam spot centre to 1.2 mm radius; at R = 2.5 mm no carbon was detected). However, there are variations in the $C^+/D^+$ flux ratios across the beam spots leading to an uncertainty of about a factor of 2 in the C/D flux ratio. (In some irradiation experiments, which were not part of this study, we noted that the central area with a diameter of ~2 mm was darker, indicating some non-uniformity of the $C^+$ beam.) During the course of the experimental measurements, the build-up of a carbon layer, which tends to protect the W from interacting with the incident $D^+$ ions, has been prevented by two means. Firstly, the $D^+$ beam was left on continuously, while the $C^+$ beam was only on for brief measurement periods (up to 200 s). Secondly, the C fraction in the beam was chosen to be low enough (~4%) so that, based on TRIDYN [13] computer simulations, for total ($D^+ + C^+$) fluences at or below $\sim 10^{23}\ m^{-2}$ no carbon overlayer is formed. Typically, $C^+$ fluences during the experiments were below $10^{21}\ m^{-2}$. According to TRIDYN simulations, the C concentration in the surface grows from 0 to ~2 at.% and the sputtering and reflection coefficients stay constant in this fluence range. Therefore, we assume that the depth profiles shown in Fig. 1 are 'quasi' steady-state profiles.

The $CD_4$ production rate was measured with an *Extranuclear* quadrupole mass spectrometer (QMS) using residual gas analysis (RGA) – the mass-20 signal was monitored. Wall contributions to the mass-20 signal (e.g., $D_2O$) were separated from the $CD_4$ signal by turning the $C^+$ beam on and off while leaving the $D^+$ beam on; typical time traces are shown in Fig. 2. (We note that exposing the specimen to $C^+$ alone, without $D^+$, did not result in any noticeable increase in the $CD_4$ signal, implying negligible D content in the surface layer – as would be expected.) A calibrated methane leak bottle was used to derive quantitative values for the $CD_4$ production rates; these rates are plotted in Fig. 3. The scatter in the data is likely to be due to variations in the ion beam fluxes, causing variations in the $C^+/D^+$ flux ratio, which in turn affects the C content of the mixed-material surface. We note, however, that the so-derived $CD_4$ production rate still includes beam-related $CD_4$ contributions that do not directly originate from the specimen surface. Rather, they might be formed at the walls, involving reflected and physically sputtered C and reflected D from the specimen; see Section 3 for details.

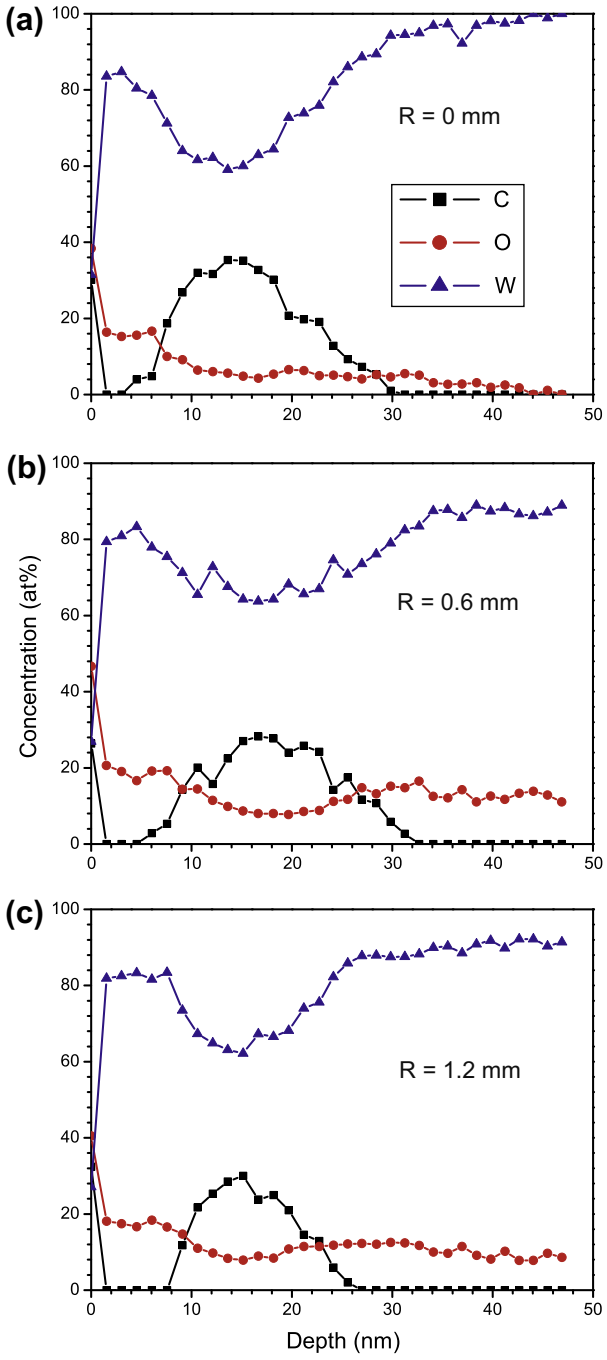


**Fig. 1.** Post-irradiation XPS depth profiles for the specimen, with the last irradiation being performed at 700 K with 6 keV $C^+$ ($7.8 \times 10^{19}\ C^+/m^2$) and 400 eV $D^+$ ($1.8 \times 10^{21}\ D^+/m^2$). Analysis locations at: (a) the centre of the beam spot, (b) at radius $R$ = 0.6 mm, and (c) at $R$ = 1.2 mm. At $R$ = 2.5 mm no C was detected and is not shown here.

Post-irradiation ex situ visual observation of the surface has shown that there was no darkening of the beam spot, confirming the absence of a deposited protective carbon overlayer, and this has been confirmed by XPS measurements shown in Fig. 1. There-

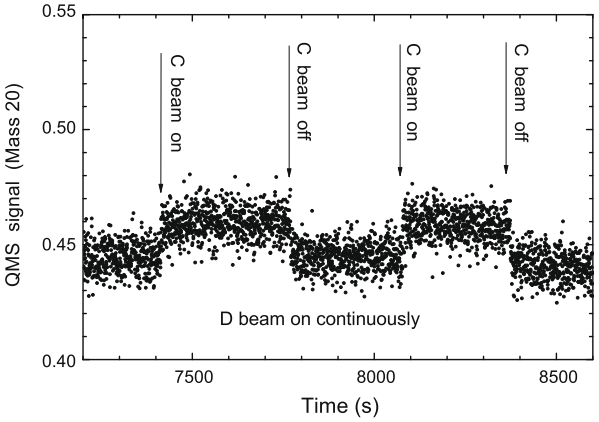


**Fig. 2.** Example of a time trace of the mass-20 QMS signal. Arrows denote the times when the $C^+$ beam was switched *on* and *off*. The $D^+$ beam was on during the whole time.

fore, the incident $C^+$ and $D^+$ ions would have interacted with a mixed W–C–D surface, rather than with a hydrogenated C–D surface. At the experimental temperatures of <900 K, we would not expect C depletion from the surface due to C diffusion into the bulk. This has been also confirmed by the XPS C depth profiles in Fig. 1. (The onset of C diffusion into W occurs at temperatures of 800–1200 K [14].)

## 3. Results and discussion

The main results of this study are the observed energy and temperature dependence of the $CD_4$ production rates measured during simultaneous irradiation of a mixed W–C–D surface with $C^+$ and $D^+$. The fact that temperature-dependent features are apparent in Fig. 3 confirms the occurrence of chemical erosion from the mixed-material surface. In general, all of the methane production curves exhibit the highest rates at room temperature (RT) followed by a decreasing trend with increasing temperature to ~500 K, followed by a levelling off at higher temperatures. The temperature dependence behaviour is quite similar for the 100 and 200 eV/$D^+$ irradiations, while for 400 eV/$D^+$ a pronounced difference is noted.

In spite of the scatter in the data, an increased level of $CD_4$ production is evident at around 320–370 K for all three energies. For temperatures >500 K, the $CD_4$ production was relatively independent of temperature for the 100 and 200 eV/$D^+$ cases. Unfortunately, our interpretation of the *flat* segment is hindered by the fact that we cannot readily separate the specimen- and wall-related contributions to the measured $CD_4$ production. (We plan to do this in future studies using line-of-sight QMS detection.) The fact that the *flat* segment is independent of temperature *might* suggest that it is dominated by wall contributions.

However, for the 400 eV/$D^+$ case, we note that the >500 K behaviour differs from the lower energy cases in that higher methane yields were observed when the specimen temperature was progressively increased, than when the specimen temperature was progressively decreased – in fact, indicating of an hysteresis effect. Since the observed hysteresis is a consequence of changing the specimen temperature, at least the difference between the two levels is directly attributable to chemical reactions on the specimen. Such an hysteresis has previously been observed during the chemical erosion of C by $H^+$ ions [15]. This is likely related to a super-saturation of deuterium in the near surface upon raising the surface temperature. A similar process may take place here, with the energy dependence related to the range, and hence to the amount of D retained in the W/WC surface layer.

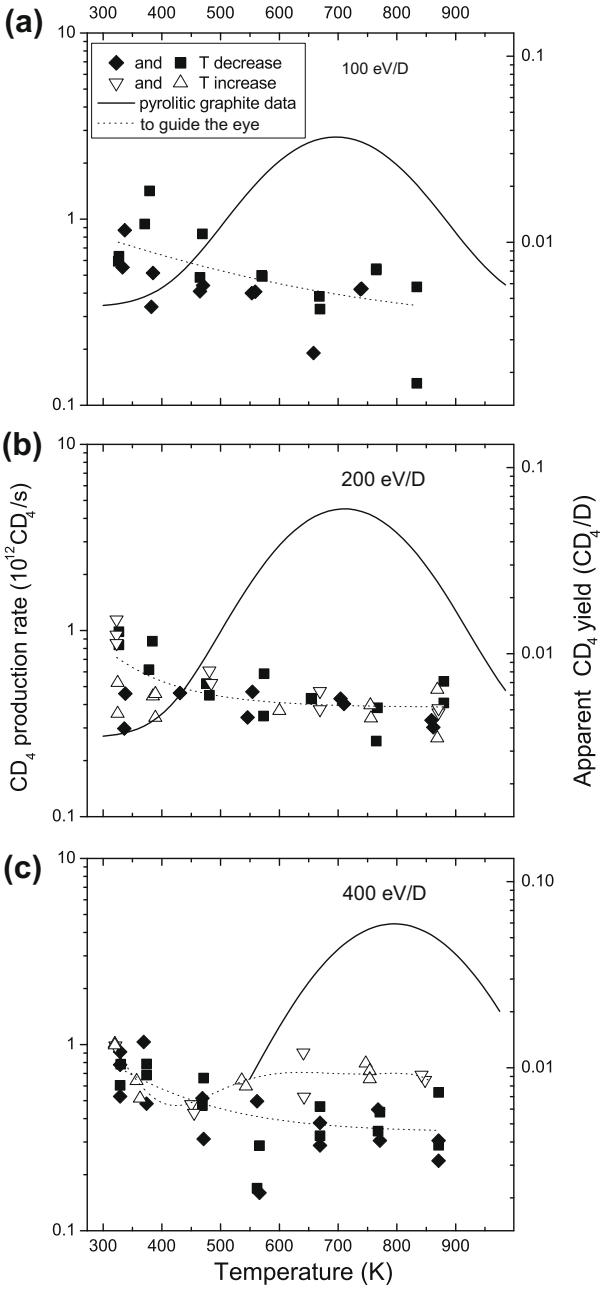


**Fig. 3.** $CD_4$ production rate as a function of specimen temperature for simultaneous bombardment of the W specimen with 6 keV $C^+$ and $D^+$ with different energies: (a) 100 eV/$D^+$, (b) 200 eV/$D^+$, and (c) 400 eV/$D^+$. Open symbols correspond to experiments where the temperature was progressively increased from 300 to 900 K, and solid symbols correspond to decreasing temperature. Symbols of the same shape represent data obtained on the same day. The scale on the right ordinates corresponds to 'apparent' yields based on assumptions discussed in the text. Methane yields for pure carbon are shown for comparison [16] for (a and b) and [17] for (c). The dotted line, included to guide the eye, is the least square fit of the averaged data at a particular temperature.

In order to compare the present $CD_4$ production levels with published methane yields for graphite, we shall normalize the measured production rates by the $D^+$ flux incident on the specimen. We note that the so-derived 'apparent' yield is over-estimated due to the inclusion of possible wall contributions. (An 'apparent' yield scale is shown on the right ordinates in Fig. 3.) Nevertheless, even if the *flat* segments in Fig. 3(a and b) and the lower *flat* segment in Fig. 3(c) were to be totally attributed to wall

contributions, the incremental yields above these levels could be attributed to chemical reactions on the specimen – giving lower-limit estimates. Based on this assumption, the magnitude of the near-RT yields and the hysteresis-related yields appear to be approximately $5 \times 10^{-3}$ $CD_4/D^+$. It is evident from Fig. 3 that the temperature dependence of $CD_4$ production obtained in this study differs from published yields for pure carbon [16,17]. While the 'apparent' yields are approximately equal to those of pure graphite at RT, the normally seen graphite peak at ~750 K is not present. This is another confirmation that we have not built up a carbon overlayer on top of the mixed W–C–D surface.

The RT high levels followed by a decreasing trend were also observed by Balden et al. [9] for single-beam $D^+$ irradiation of W-doped magnetron deposited C layers with low W concentrations (2.8–14.5 at.%). In their case, the RT yield was ~2.5%, which is somewhat higher than observed in our experiments. It is not evident at this time whether the yield difference might be attributable to the different C/W fractions in the respective experiments. In their case the C concentration was very high (85–97%) while in ours the C concentrations were relatively low (~4%).

After the irradiation experiments the specimen was removed from the irradiation test chamber and was analyzed by sputter-XPS. The depth profiles of C, O, and W concentrations for different radial locations on the beam spot are plotted in Fig. 1. The spike in C and O concentrations at the very surface is explained by contamination during transfer in air. The presence of both C and W within the top 30 nm signifies the mixed W–C layer. The XPS profiles clearly show that C has been depleted for depths up to ~8 nm. This depletion may be due to both physical and chemical processes, as the $D^+$ mean projectile range in W is ~7 nm as calculated by TRIDYN [13]. However, we do not have sufficient information to separate the contributions of these effects. It has been also confirmed that the maximum C depth is ~30 nm. Therefore, the entire implanted C is within the projectile range and there is no diffusion of C into the bulk in our experiments. The similar depth profiles taken from different radial positions on the beam spot (Fig. 1) confirm that no carbon overlayer has been formed. Thus, the $CD_4$ emission must have originated from the mixed W/C surface. We would also expect the C profile shapes to vary with radial locations due to possible variations in the local C/D flux ratio due to beam non-uniformity. However, the observed similarity in the C profiles implies that the flux ratios are reasonably uniform across the beam spot.

## 4. Conclusions

The main results of this study are the observed dependence of methane production on $D^+$ energy and temperature (300–900 K) during simultaneous irradiation of a mixed W–C–D surface with $C^+$ (6 keV $C^+$) and $D^+$ (100–400 eV/$D^+$). In general, all of the methane production curves exhibit the highest rates at RT followed by a decreasing trend to ~500 K, and then levelling off for higher temperatures. The level part of the curves is attributed, at least partially, to wall contributions. The temperature dependence behaviour is quite similar for the 100 and 200 eV/$D^+$ irradiations, while for 400 eV/$D^+$ an hysteresis effect is evident depending on whether the temperature from experiment to experiment is being increased or decreased. Both the elevated methane levels at RT and the presence of a specimen-temperature-dependent hysteresis are attributable to chemical reactions on the specimen. Methane yield ($CD_4/D^+$) estimates are ~1–1.5% at RT, decreasing to 0.5% at 500 K. The XPS C profiles clearly show the depletion of C in the mixed W–C layer. This is likely to be due to a combination of physical and chemical processes. However, at present we do not have sufficient information to separate these two effects.

Therefore, for ITER-relevant temperatures the release of carbon from a W–C–D mixed surface via deuterium-induced chemical erosion might be negligible and would not adversely affect the lifetime of tungsten plasma-facing materials.

## Acknowledgements

We gratefully acknowledge the funding from the Natural Sciences and Engineering Research Council of Canada.

## References

[1] G. Janeschitz, J. Nucl. Mater. 290–293 (2001) 1.
[2] D. Meade, S.C. Jardin, J.A. Schmidt, et al., Mission and design of the fusion ignition research experiment, in: Proceedings of the 18th IAEA Conf. on Fusion Energy, Sorrento, Italy October, 2000, (CD-ROM), IAEA-CN-77/FTP2/16, IAEA, Vienna, 2001.
[3] S. Nishio, K. Ushigusa, S. Ueada, et al., Conceptional design of advanced steady-state tokamak reactor, in: Proceedings of the 18th Conf. on Fusion Energy, Sorrento, Italy October, 2000, (CDROM), IAEA-CN-77/FTP2/14, IAEA, Vienna, 2001.
[4] A.S. Kukushkin, H.D. Pacher, D.P. Coster, et al., J. Nucl. Mater. 337–339 (2005) 50.
[5] K. Schmid, K. Krieger, A. Kukushkin, A. Loarte, J. Nucl. Mater. 363–365 (2007) 674.
[6] K. Krieger, H. Maier, R. Neu, et al., J. Nucl. Mater. 266–269 (1999) 207.
[7] I. Bizyukov, K. Krieger, J. Appl. Phys. 101 (2007) 104906.
[8] K. Schmid, J. Roth, J. Nucl. Mater. 313–316 (2003) 302.
[9] M. Balden, E. de Juan Padro, I. Quintana, B. Cieciwa, J. Roth, J. Nucl. Mater. 337–339 (2005) 980.
[10] I. Bizyukov, K. Krieger, J. Appl. Phys. 102 (2007) 074923.
[11] A.A. Haasz, J.W. Davis, Nucl. Inst. Method B83 (1993) 117.
[12] W. Eckstein, Calculated Sputtering, Reflection and Range Values, IPP report 9/132, 2002.
[13] W. Moeller, W. Eckstein, J.P. Biersack, Comput. Phys. Commun. 51 (1988) 355.
[14] K. Schmid, J. Roth, W. Eckstein, J. Nucl. Mater. 290–293 (2001) 148.
[15] J. Roth, in: R. Behrisch (Ed.), Sputtering by Particle Bombardment II, Springer-Verlag, New York, 1983.
[16] B.V. Mech, A.A. Haasz, J.W. Davis, J. Nucl. Mater. 255 (1998) 153.
[17] J.W. Davis, A.A. Haasz, P.C. Stangeby, J. Nucl. Mater. 145–147 (1987) 417.